Analysis of Passive Charge Balancing for Safe Current-Mode Neural Stimulation

Luis E. Rueda G.*, Marco Ballini†, Nick Van Hellepute†, Srinjoy Mitra‡
*Universidad Industrial de Santander, Bucaramanga, Colombia
†IMEC, 75 Kapeldreef, Leuven, Belgium
‡University of Glasgow, Glasgow, UK

***Abstract*—Charge balancing has been often considered as one of the most critical requirement for neural stimulation circuits. Over the years several solutions have been proposed to precisely balance the charge transferred to the tissue during anodic and cathodic phases. Elaborate dynamic current sources/sinks with improved matching, and feedback loops have been proposed with a penalty on circuit complexity, area or power consumption. Here we review the dominant assumptions in safe stimulation protocols, and derive mathematical models to determine the effectiveness of passive charge balancing in a typical application scenario.**

***Index Terms*—Neural stimulation, charge balance, safety limits.**

I. Introduction

Peripheral nerve interfaces have recently become one of the most active field of study in chronic neural implants. A large number of possible applications from disease ailments [1] to prosthetics [2] are now investigated. Over the years, various modes of stimulation (current, voltage or charge) have been analyzed in literature and sophisticated circuits have been developed for precise charge balancing. Nonzero net charge transferred through the electrodes can have adverse effects in inducing irreversible elecrochemical reactions at the electrode interface resulting in tissue damage [3]. In most cases, active charge balancing is either done by a high precision current source/sink [4]–[6], by feedback techniques to measure charge error [7], or by using some sort of bridge network [8], [9]. While using a blocking capacitor is generally the easiest method to stop DC current flowing through the tissue [10], the size of the required capacitor is often impossible to implement in a high-density neural array. Furthermore, recent studies have shown that a blocking capacitor could be detrimental due to the unknown DC offset developed at the electrode [11].

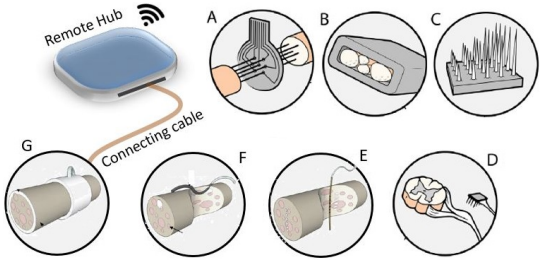

Fig. 1: Various peripheral nerve stimulation probes (adapted from [2] and [7]).

The accuracy to which charge balance is necessary is often not consistently defined over literature. One of the original numbers (below 100 nA DC current error) was cited for a cochlear implant study [12] and has been cross-cited numerous times also for other applications [5]. This number has also been used by the European cochlear implant standard [13]. In other cases, various authors have cited 25 nA DC current error (as an industry standard), or a charge error of 15 nC [4] to be the safe limit. Nevertheless, most recent publications aim to achieve DC current or charge errors which are way less than these numbers. This may result in over design, potentially limiting the possibility of scaling to high-density neural arrays where electrodes and corresponding circuits have to fit within a very small area (e.g. $<100\,\mu$m electrode pitch).

Other authors consider a limit on the electrode-electrolyte potential, which should be kept within the water window, to avoid irreversible faradaic reactions start taking place [3]. The water window depends largely on electrode material, e.g., $[-0.6\,\text{V},\ 0.8\,\text{V}]$ (with respect to a Ag-AgCl reference electrode) for Pt and IrOx, and $[-0.9\,\text{V},\ 0.9\,\text{V}]$ for TiN [3]. However, much smaller windows are often considered for safety (e.g., $\pm100\,$mV [7], or $\pm50\,$mV [14]). Though some implementations that aim at controlling the electrode potential already exist [7], [15], this approach is not as common as those that try to limit the DC current. However, as indicated in [3], it might be not only easier but also desirable to design pulse generators that avoid exceeding the water window, rather than those which ensure the stimulus is precisely charge-balanced.

In this analysis we consider the case of passive charge balancing scheme to determine the boundary conditions of safe stimulation for both the electrode voltage and the current injected into tissue.

II. Stimulation Setup

Fig. 1 shows various methods of peripheral nerve stimulation that have become possible over the last decade. Active high-density electrode arrays are expected to be placed very close to the nerve fibers and connected to a subcutaneous or external remote hub. Since the electrodes are placed in close proximity to the nerve fibres, the required current magnitude for eliciting an action potential is expected to be within 100 μA (much smaller than typical muscular excitation and cochlear implants). The charge per phase ($\sim$10-20 nC) and stimulation frequency ($<100\,$Hz) typically required in this case can be

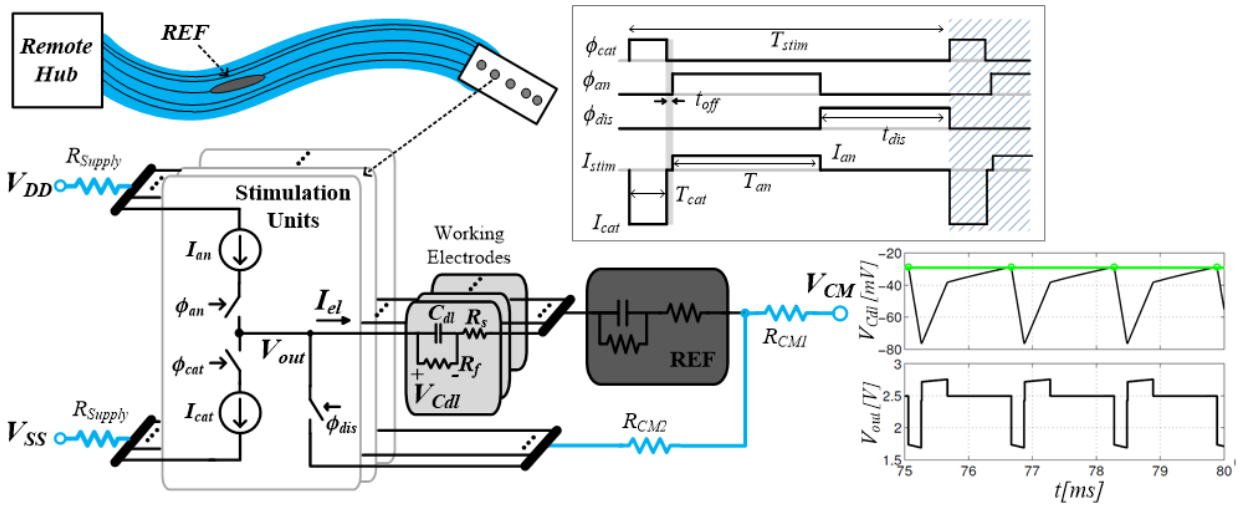

Fig. 2: A generic tethered probe and simplified current-mode stimulation circuit (with passive discharge) is shown on the left. The stimulation timing diagram, and resulting (quasi-static) voltage waveforms are shown in inset. Here V_{CM} is set to mid-supply voltage (2.5V).

found, e.g., in [16]. In Fig. 2, a generic tethered probe is shown, with simplified schematics for the stimulation units and the electrode model. Timing diagram of the output current and voltage waveforms are shown in inset. In the remainder of this paper, we employ a common first-order approximation for the electrode model, consisting of a double-layer capacitance C_{dl} and a charge transfer resistance R_f. The tissue resistance is modeled by the spreading resistance R_s. For more accurate models, please refer to [17] or [3]. It is assumed that a large reference electrode ($>10\times$ stimulating electrode) biases the body (at $\sim V_{CM}$) while none of the voltage sources (V_{DD}, V_{SS} or V_{CM}) are within close proximity of the electrodes.

III. Analysis of Electrode Voltage and Current Safe Limits

Biphasic neural stimulation that lasts for a sustained amount of time is considered in the following analysis. Here we consider the case of multiple subsequent biphasic pulses, each followed by a discharge phase of finite duration, achieved shorting the electrode to the reference voltage V_{CM}. This technique is known as passive discharge. Since the discharge is not complete, residual charge accumulates at the double layer capacitance and a voltage builds up across the electrode-electrolyte interface. However, as will be shown below, eventually a periodic steady-state ("quasi-static") condition is reached. In the following, we derive the instantaneous and final voltages as well as the current injected into the body. A similar analysis was shown in [18], where a simplifying assumption was made that the discharge phase is much shorter than the electrode time constant. As a consequence, the discharge current was considered constant during the whole discharge phase. In [7], a refined formula is obtained, by introducing an exponential term in the expression of the electrode voltage after discharge, but the underlying assumptions and the limits of validity are not clearly stated.

A. Quasi-Static Electrode Voltage

At each biphasic stimulation, the net charge (Q_{error}) injected into the electrode could be nonzero, mainly due to mismatches in the anodic and cathodic currents. Since the charge in the anodic and cathodic phase are nominally equal, we can write $I_{cat} = \alpha(I_{an} \pm \Delta I_{an}) = \alpha I_{an} \pm \Delta I_{cat}$, where I_{an}, I_{cat} and T_{an}, T_{cat} have their usual meaning as shown in Fig. 2, and $\alpha = T_{an}/T_{cat}$. Then, the charge error can be expressed as:

$$Q_{error} = \pm\Delta I_{an} \cdot T_{an} = \pm\Delta I_{cat} \cdot T_{cat} = \pm\Delta I \cdot T_{ph}. \quad (1)$$

If passive discharging of the electrode is used after each biphasic pulse, at the end of the discharge phase some residual charge will still be present on the double layer capacitor (C_{dl}). After the first stimulation and discharge cycle, the residual charge will be:

$$Q_d[n=1] = Q_{error} e^{-t_d/\tau_e}, \quad (2)$$

where t_d is the duration of the discharge phase and $\tau_e = [(R_s + R_{dis}) \| R_f] C_{dl}$ is the discharge time constant.[1] Since the discharge is not complete, the charge at the electrode accumulates, and the residual charge at the end of the n-th discharge phase will be depending on the residual charge of the previous phase:

$$Q_d[n] = (Q_d[n-1] + Q_{error}) e^{-t_d/\tau_e}. \quad (3)$$

[1]Here R_{dis} includes all the resistances in the discharge path: the on-resistance of the discharge switch, the wire resistance R_{CM2}, as well as the spread resistance of the reference electrode. The double layer capacitance of the reference electrode is neglected, because in many applications this electrode has a very large area compared to the stimulation electrodes. We also assume that the charge leaked through R_f during the stimulation phases ($T_{an} + T_{cat}$) is negligible, due to the very large time constant $R_f C_{dl}$.

Solving the previous difference equation for $Q_d[0] = 0$, the residual charge at the end of the discharge phase of the n-th stimulation period can be obtained as:

$$Q_d[n] = Q_{error}\left(\frac{1 - e^{-n \cdot t_d/\tau_e}}{1 - e^{-t_d/\tau_e}}\right)e^{-t_d/\tau_e}, \quad (4)$$

As can be noted from (2), the discharge becomes faster when the accumulated charge increases. Eventually a periodic steady state is reached, where the residual charge is equal to the previous cycle (i.e., $Q_{d\infty} = Q_d[n] = Q_d[n-1]$ for $n \to \infty$), and the quasi-static charge at the end of the discharge phase is given by:

$$Q_{d\infty} = Q_{error}(e^{t_d/\tau_e} - 1)^{-1}. \quad (5)$$

The voltage across the electrode-electrolyte interface after each discharge phase is then given by:

$$V_{C_{dl}}[n] = Q_d[n]/C_{dl}. \quad (6)$$

This accumulated offset obviously adds up to both the voltage *at* the electrode (i.e., at the output of the current source), V_{out}, and to the voltage *across* the electrode-electrolyte interface, $V_{C_{dl}}$. The first, V_{out}, is relevant for the operation of the stimulation circuit, and must be kept within the compliance range limits of the current source. The second, $V_{C_{dl}}$, does not include the IR drop in the tissue and, although not accessible for direct measurement, is relevant for reversible charge injection, where a limit is imposed by the water window [19].[2] Substituting equations (5) in (6), the quasi-static electrode voltage can be obtained as:

$$V_{C_{dl}\infty} = \frac{Q_{error}}{C_{dl}}\left(\frac{1}{e^{t_d/\tau_e} - 1}\right). \quad (7)$$

From equations (1) and (7), it is possible to derive the maximum mismatch error, that can be tolerated between the cathodic an anodic currents, to maintain $V_{C_{dl}\infty}$ within a desired limit:

$$\text{error}_I = \frac{\Delta I}{I_{ph}} = \frac{Q_{error}}{Q_{ph}} = \frac{C_{dl}V_{C_{dl}\infty}}{Q_{ph}}(e^{t_d/\tau_e} - 1), \quad (8)$$

where Q_{ph} is the nominal charge per phase ($Q_{ph} = I_{an} \cdot T_{an} = I_{cat} \cdot T_{cat} = I_{ph}T_{ph}$). With the approximations considered here, the maximum voltage across the electrode is given by $V_{C_{dl}\infty} + Q_{ph}/C_{dl}$, and to maintain it within a limit $V_{C_{dl}max}$ imposed by the water window, the tolerable current mismatch is then given by:

$$\text{error}_I = \frac{C_{dl}V_{C_{dl}max} - Q_{ph}}{Q_{ph}}(e^{t_d/\tau_e} - 1), \quad (9)$$

[2]For a more general description of the maximum polarization across the electrode-electrolyte, please refer to [3].

B. Average (DC) Current

Let us define the safe value for a net DC current $I_{DC_{safe}}$. Taking into account that for multi-electrode stimulation, N_e electrode units could be stimulating simultaneously, the sum of charge errors should be limited to (referring to Fig. 2):

$$\sum_{i=1}^{N_e} Q_{e_i} \leq I_{DC_{safe}} \cdot T_{stim}, \quad (10)$$

where Q_{e_i} is the remaining charge error after one complete stimulation period (i.e. including the discharge phase). Q_{e_i} is composed of the net charge injected into the tissue during stimulation ($Q_{e_{stim,i}} = Q_{error_i}$), and of $Q_{e_{dis,i}}$, which is the charge injected into the tissue during the discharge phase:

$$Q_{e_i} = Q_{e_{stim,i}} + Q_{e_{dis,i}} = Q_{error_i} + \frac{R_f \cdot Q_{dis_i}}{R_f + R_s + R_{dis}}, \quad (11)$$

where $Q_{dis_i} = Q_{d_i}[n] - (Q_{d_i}[n-1] + Q_{error_i})$ is the charge removed from C_{dl} during the discharge phase. Then, from equations (4), (10) and (11), the average current per stimulation cycle can be obtained as:

$$I_{DC}[n] = \sum_{i=1}^{N_e} \frac{Q_{error_i}}{T_{stim}}\left(\frac{\tau_e}{R_f C_{dl}} + \frac{R_f \cdot e^{-n \cdot t_d/\tau_e}}{R_f + R_s + R_{dis}}\right). \quad (12)$$

Hence, for $n \to \infty$ the average current per cycle t is:

$$I_{DC} = \sum_{i=1}^{N_e} \frac{Q_{error_i}}{T_{stim}}\left(\frac{R_s + R_{dis}}{R_f + R_s + R_{dis}}\right). \quad (13)$$

It can be readily verified that without including the faradaic resistance, the average current per cycle reaches zero at the quasi-static condition. As stated in equation (1), $Q_{error_i} = \Delta I_i \cdot T_{ph}$, and by assuming ΔI_i as a zero mean uncorrelated stochastic variable with standard deviation σ_I:

$$\left|\sum_{i=1}^{N_e} \Delta I_i\right| = \sqrt{\sum_{i=1}^{N_e} \sigma_I^2} = \sqrt{N_e} \cdot \sigma_I \quad (14)$$

Substituting equations (14) and (1) in (13), one could obtain an expression for the tolerable relative mismatch error between the cathodic and anodic currents σ_I/I_{ph}, to maintain the average (DC) current within a desired limit $I_{DC_{safe}}$:

$$\text{error}_I = \frac{\sigma_I}{I_{ph}} = \frac{I_{DC_{safe}}}{\sqrt{N_e}} \cdot \frac{T_{stim}}{Q_{ph}} \cdot \left(1 + \frac{R_f}{R_s + R_{dis}}\right). \quad (15)$$

C. Application Example

In this section an example with actual electrode and stimulation parameters is presented. We considered a $120 \times 120\,\mu\text{m}^2$ IrOx stimulation electrode that has $C_{dl} = 420\,\text{nF}$, $R_s = 7.35\,\text{k}\Omega$, $R_f = 2.3\,\text{M}\Omega$, and $R_{dis} = 1\,\text{k}\Omega$. The stimulation parameters used are quite typical for peripherial nerve application [16]: $Q_{ph} = 20\,\text{nC}$, $T_{cat} = 200\,\mu\text{s}$, $T_{an} = 400\,\mu\text{s}$, $t_d = 1$ ms. We also consider $\Delta I/I_{ph} = 20\%$. For simplicity, only one stimulation unit was assumed ($N_e = 1$). The transient electrode voltage and the average DC current at the end of each discharge phase, derived from equations (4)-(6) and

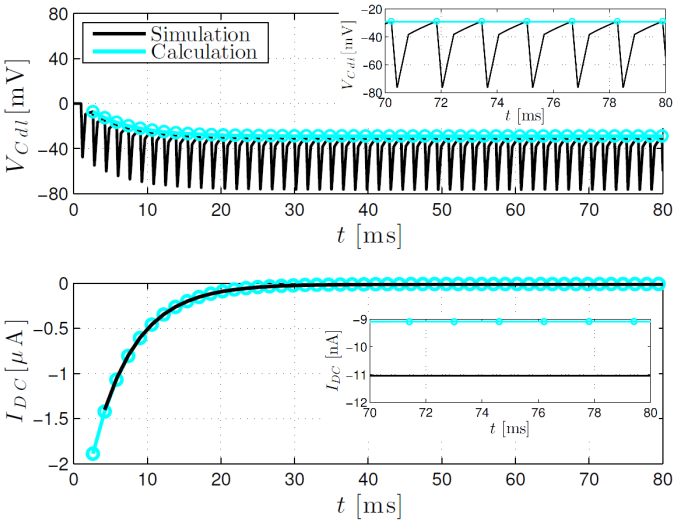

Fig. 3: Comparison between the calculations and simulations of the quasi-static electrode voltage (top) and average DC current (bottom).

(12), are shown in Fig. 3 and compared with simulation results. As it can be observed, after few stimulation cycles the electrode voltage reaches a quasi-static condition (29 mV) and the average current per cycle decreases to a negligible value (-11 nA), even for huge mismatch between the anodic and cathodic currents (20%). The latter can be explained with Fig. 4, where curves of the tolerable mismatch errors are calculated with respect to the discharge time, from equations (8) and (15). It can be noted that for the electrode parameters above,

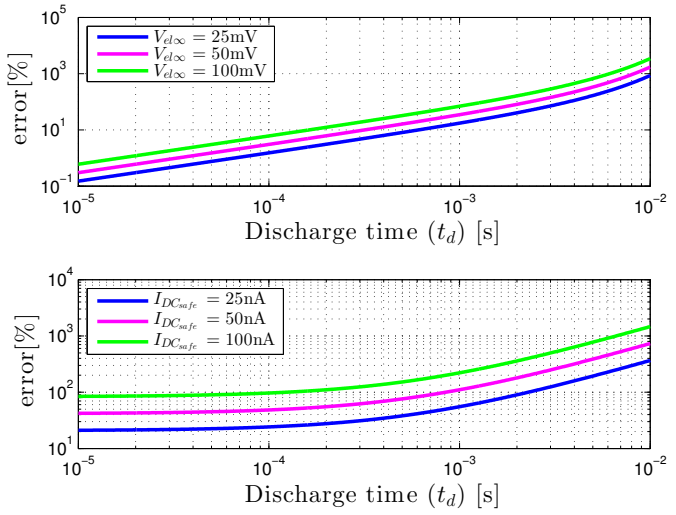

Fig. 4: Tolerable mismatch between I_{an} and I_{cat} to maintain $V_{C_{dl\infty}}$ within 25 mV, 50 mV and 100 mV (top), and I_{DC} within $I_{DC_{safe}}$, for 25 nA, 50 nA, 100 nA (bottom), for $Q_{ph} = 40$ nC.

the matching conditions between the stimulation currents are very relaxed ($> 17\%$) for discharge times longer than 1 ms ($\sim 0.3\tau_e$), when a limit for $V_{C_{dl}\infty}$ of ± 100 mV is considered. When the limits on the average current are instead considered, the mismatch conditions are even more relaxed, and higher errors are allowed for discharge times longer than 1 ms ($> 55\%$). In this case the stimulation frequency ($1/T_{stim}$) can be up to $\sim$625 Hz, well within the requirement for peripheral nerve stimulation.

IV. Conclusion

In this paper a general analysis of charge and current errors occurring from simple passive discharge mechanism in a neural stimulation is reported. To the best of our knowledge, this is the most comprehensive analysis till date. The equations given in this paper indicate how much mismatch can be tolerated and can serve the reader to identify whether passive discharge is sufficient for their specific application, or instead other approaches are necessary. With realistic parameters for the electrode and the stimulation protocol, we showed that passive discharge can be sufficient to maintain the electrode voltage and DC current within safe limits for a wide range of conditions.

References

[1] K. Famm *et al.*, "Drug discovery: A jump-start for electroceuticals," *Nature*, 2013.

[2] H. P. Saal *et al.*, "Biomimetic approaches to bionic touch through a peripheral nerve interface," *Neuropsychologia*, 2015.

[3] S. F. Cogan, "Neural stimulation and recording electrodes," *Annu. Rev. Biomed. Eng.*, 2008.

[4] J. J. Sit *et al.*, "A Low-Power Blocking-Capacitor-Free Charge-Balanced Electrode-Stimulator Chip With Less Than 6nA DC Error for 1mA Full-Scale Stimulation," *IEEE Trans. Biomed. Circuits Syst.*, 2007.

[5] H. Chun *et al.*, "Safety ensuring retinal prosthesis with precise charge balance and low power consumption," *IEEE Trans. Biomed. Circuits Syst.*, 2014.

[6] Z. Luo *et al.*, "A High-Voltage-Tolerant and Precise Charge-Balanced Neuro-Stimulator in Low Voltage CMOS Process," *IEEE Trans. Biomed. Circuits Syst.*, 2016.

[7] K. Sooksood *et al.*, "An active approach for charge balancing in functional electrical stimulation," *IEEE Trans. Biomed. Circuits Syst.*, 2010.

[8] X. Liu *et al.*, "An integrated implantable stimulator that is fail-safe without off-chip blocking-capacitors," *IEEE Trans. Biomed. Circuits Syst.*, 2008.

[9] S. Nag *et al.*, "Flexible charge balanced stimulator with 5.6 fc accuracy for 140 nc injections," *IEEE Trans. Biomed. Circuits Syst.*, 2013.

[10] M. Ortmanns, "Charge Balancing in Functional Electrical Stimulators: A Comparative Study," *IEEE ISCAS*, 2007.

[11] M. N. van Dongen *et al.*, "Does a coupling capacitor enhance the charge balance during neural stimulation? an empirical study," *Medical & Biological Engineering & Computing*, 2016.

[12] R. K. Shepherd *et al.*, "Chronic electrical stimulation of the auditory nerve using non-charge-balanced stimuli," *Acta Otolaryngol.*, 1999.

[13] CENELEC, *Active implantable medical devices - Part 2-3*. EN 45502-2-3, 2010.

[14] E. Maghsoudloo *et al.*, "A new charge balancing scheme for electrical microstimulators based on modulated anodic stimulation pulse width," *IEEE ISCAS*, 2016.

[15] N. Butz *et al.*, "A 22V Compliant 56uW Active Charge Balancer Enabling 100% Charge Compensation Even in Monophasic and 36% Amplitude Correction in Biphasic Neural Stimulators," *IEEE ISSCC*, 2016.

[16] S. Raspopovic *et al.*, "Restoring Natural Sensory Feedback in Real-Time Bidirectional Hand Prostheses," *Sci. Transl. Med.*, 2014.

[17] W. Franks *et al.*, "Impedance characterization and modeling of electrodes for biomedical applications." *IEEE Trans. Biomed. Eng.*, 2005.

[18] K. Sooksood *et al.*, "An experimental study on passive charge balancing," *Adv. Radio Sci.*, 2009.

[19] T. Rose *et al.*, "Electrical stimulation with Pt electrodes. VIII. Electrochemically safe charge injection limits with 0.2 ms pulses (neuronal application)," *IEEE Trans. Biomed. Eng.*, 1990.